JOURNAL OF VIROLOGY, July 1979, p. 156-171
0022-538X/79/07-0156/16$02.00/0

Vol. 31, No. 1

Restriction Cleavage Map of SP01 DNA: General Location of Early, Middle, and Late Genes

JANICE PERO,* NANCY M. HANNETT, AND CAROL TALKINGTON

The Biological Laboratories, Harvard University, Cambridge, Massachusetts 02138

Received for publication 20 December 1978

A detailed restriction endonuclease map for the genome of *Bacillus subtilis* phage SP01 is presented. Sites of cleavage for the restriction enzymes *Bgl*II, *Eco*RI*, *Hae*III, and *Sal*I were determined. This physical map showed that SP01 DNA was 140 kilobases in length and contained a repeated sequence of 12.4 kilobases at its termini. Combined with previously published information, we were also able to identify the general locations of genes expressed at early, middle, or late times in the phage lytic cycle. In particular, early genes were largely clustered in the terminal repeats, whereas a major cluster of late genes was located in the left-central portion of the genome.

Bacteriophage SP01 is a large, virulent phage of *Bacillus subtilis* with a double-stranded DNA genome of about 10^8 daltons (13). Although little is known about the organization of genes on the SP01 genome, a large collection of nonsense mutations of the phage have been divided into 36 cistrons and ordered to yield a linear map (2, 14). Three of these cistrons (*28*, *33*, and *34*) define regulatory genes which control the well-defined temporal program of SP01 gene expression (6). Gene *28*, whose product is required for middle RNA synthesis, specifies a regulatory subunit of the host RNA polymerase (RNA nucleotidyltransferase) that acts in place of sigma factor to direct binding and initiation at middle promoters on the phage DNA (3, 5, 19). The gene *33* and gene *34* products also bind to the bacterial RNA polymerase and direct this enzyme to recognize the late genes of SP01 (4, 21). The finding that modified forms of RNA polymerase recognize different temporally defined classes of promoters has prompted us to investigate the location of early, middle, and late genes and their promoters.

The restriction endonucleolytic activity *Eco*RI* cleaves SP01 DNA into 27 fragments. In a previous study, we identified the temporal classes of genes contained on each of these fragments by hybridization with in vivo- and in vitro-synthesized RNAs (18). Here, we report the order of these fragments and, hence, the general locations of early, middle, and late phage genes on the SP01 genome.

MATERIALS AND METHODS

Preparation of SP01 DNA. Wild-type *B. subtilis* strain NCTC 3610 was infected with wild-type SP01, obtained from D. Shub. Phage were grown and purified as described previously (18). SP01 DNA was extracted with phenol from the purified wild-type phage.

Restriction reactions. *Eco*RI restriction endonuclease was purified as described previously (18). SP01 DNA and *Eco*RI endonuclease (10 U/μg of SP01 DNA) were incubated for 2 h under optimal conditions for *Eco*RI* activity (15, 18). *Tha*I (*Tac*I) restriction endonuclease, a gift from D. McConnell, was incubated with SP01 DNA for 1 h at 60°C in 10 mM Tris-hydrochloride (pH 7.4)-1 mM EDTA-10 mM $MgCl_2$. *Sma*I restriction endonuclease, purified at the Cold Spring Harbor Laboratory (Cold Spring Harbor, N. Y.) by C. Mulder, was incubated with SP01 DNA for 1 h at 30°C in 50 mM Tris-hydrochloride (pH 9.0)-15 mM KCl-5 mM $MgCl_2$. Other restriction endonucleases used to digest the SP01 genome were purchased from either New England Biolabs (Beverly, Mass.) or Bethesda Research Laboratories, Inc. (Rockville, Md.); the assay conditions described for the enzymes were used except that we substituted 1 mM dithiothreitol for β-mercaptoethanol. Table 1 details the amounts (units) of restriction enzymes used per microgram of SP01 DNA. All reactions were carried out for 4 h, with the following exceptions: *Bgl*II, 6 h; *Bst*EII, *Hae*II, *Hae*III, *Hha*I, and *Kpn*I, 2 h. After restriction, DNA fragments were extracted with phenol, extracted with ether, precipitated by ethanol, and suspended in 10 mM Tris-hydrochloride (pH 7.5)-1 mM EDTA.

Double digestion of the SP01 genome by two restriction enzymes was accomplished by restricting the DNA with the first enzyme; the resultant digest was phenol extracted and ethanol precipitated, and these SP01 DNA fragments were then submitted to the action of the second restriction endonuclease.

All restriction digestion patterns were analyzed by agarose gel electrophoresis as described previously (18).

Radioactive labeling of restriction fragments. For radioactive labeling of restriction fragments, the reaction mixture (100 μl) contained 20 mM Tris-hydrochloride, pH 7.4; 5 mM $MgCl_2$; 1 mM dithiothreitol,

10 μM each dCTP, dGTP, and dTTP; 1 μM [α-^{32}P]-dATP (specific activity, 300 Ci/mmol); 1 to 3 μg of SP01 DNA restriction fragments; and 0.5 U of DNA polymerase I (Miles Laboratory Research Products, Elkhart, Ind.) (DNA nucleotidyltransferase). After a 15-min incubation at 15°C, the fragments (approximately 1×10^6 to 4×10^6 cpm/μg) were extracted with phenol, precipitated by ethanol, and suspended in loading buffer (4 mM Tris-hydrochloride (pH 7.8), 0.5 mM sodium acetate, 0.1 mM EDTA, 0.01% bromophenol blue). (In some experiments, we used SP01 DNA radioactively labeled in vivo by growth of the phage on [^{32}P]phosphate.)

Hutchison procedure for mapping DNA restriction fragments. The following procedure for mapping DNA restriction fragments was designed by C. Hutchison (16; personal communication).

(i) Cold dimension. SP01 DNA restriction fragments (20 to 25 μg) were loaded across the top of a 0.7% agarose slab gel (16 by 21 cm), separated by electrophoresis, and transferred onto a sheet of nitrocellulose by the procedure developed by Southern (17), as described previously (18). The filter was air dried for at least 5 h and subsequently baked in a vacuum oven at 80°C for 3 h.

(ii) Radioactive dimension. SP01 DNA (1 to 3 μg) was digested by a second restriction enzyme and then labeled with [α-^{32}P]dATP as described above. This ^{32}P-labeled restriction digest (4×10^6 to 8×10^6 cpm) was loaded onto a second agarose slab gel, and the fragments were separated by electrophoresis.

(iii) Transfer and annealing. SP01 [^{32}P]DNA fragments were denatured by soaking the agarose gel in 0.5 N NaOH–0.9 M NaCl for 1 h and then neutralized in 1.0 M Tris-hydrochloride (pH 7.4)–0.9 M NaCl–0.1% sodium dodecyl sulfate for 1 h. These DNA fragments were then transferred onto the same nitrocellulose sheet that contained the cold dimension. The agarose gel was positioned so that its [^{32}P]DNA band pattern was rotated 90° with respect to the cold DNA band pattern imprinted on the filter; thus, each unlabeled fragment of the first digest could intersect each radioactive restriction fragment of the second digest.

The transfer of the radioactive fragments from the gel to the filter was accomplished according to the Southern technique, except (i) the transfer buffer was 4× SSC (1× SSC = 0.15 M NaCl plus 0.015 M sodium citrate)–0.1% sodium dodecyl sulfate and (ii) the procedure was carried out in a 66°C environmental chamber. Thus, the SP01 [^{32}P]DNA fragments stuck to the filter only at points of intersection between two DNA bands containing homologous sequences. The remaining labeled DNA passed through the filter and was trapped in paper towels. Upon completion of the transfer (20 h), the nitrocellulose filter was washed at 66°C in transfer buffer for 1 h and then was submitted to three 20-min rinses in 3 mM Tris base (at room temperature). Points of DNA-DNA annealing between the unlabeled and labeled digests were visualized by placing the air-dried filter against X-ray film (Kodak SB5).

RESULTS

Restriction endonuclease cleavage of SP01 DNA. SP01 DNA contains the unusual base 5-hydroxymethyluracil in place of thymine (13). We tested the ability of 22 different restriction enzymes to cleave SP01 DNA (Table 1). A number of the enzymes cleaved 5-hydroxymethyluracil-containing SP01 DNA as efficiently as they cleaved thymine-containing λ DNA. Three of these restriction endonucleases (*Hpa*II, *Hha*I, and *Hae*III) have only guanine·cytosine base pairs in their recognition sites, and hence the presence of 5-hydroxymethyluracil would not be expected to affect their activity; however, others, such as *Sal*I and *Alu*I, which contain adenine·thymine base pairs in their recognition sites also worked efficiently on SP01 DNA. A number of other restriction enzymes cleaved the phage DNA completely only when excess quantities of enzyme were used (*Eco*RI*, *Kpn*I, and *Hae*II), whereas other enzymes failed to cleave the 5-hydroxymethyluracil-containing DNA or produced what appeared to be incomplete digests (see Table 1).

The restriction enzymes *Bgl*II, *Hae*III, and *Sal*I had the fewest cleavage sites in SP01 DNA; *Sal*I cleaved SP01 DNA into five fragments, whereas *Bgl*II and *Hae*III each generated six

TABLE 1. *Cleavage of SP01 DNA with restriction endonucleases*

Enzyme	Sequence[a]	No. of cleavage sites	U/μg of DNA[b]
*Alu*I	AG↓CT	>100	1
*Ava*I	C↓PyCGPuG	0	8
*Bam*HI	G↓GATCC	0	9
*Bgl*II	A↓GATCT	5	2
*Bst*EII	Unknown	25–35	3
*Eco*RI	G↓AATTC	26	10
*Hae*II	PuGCGC↓Py	25–35	3
*Hae*III	GG↓CC	5	1
*Hha*I	GCG↓C	>40	1
*Hinc*II	GTPyPuAC	P[c]	10
*Hind*III	A↓AGCTT	P	20
*Hin*fI	G↓ANTC	>100	4
*Hpa*II	C↓CGG	>40	1
*Kpn*I	GGTAC↓C	20–30	5
*Pst*I	CTGCA↓G	0	6
*Sal*I	G↓TCGAC	4	1
*Sau*3A	↓GATC	>100	2
*Sma*I	CCC↓GGG	0	4
*Sst*I	GAGCT↓C	0	2
*Tac*I	CG↓CG	0	6
*Xba*I	T↓CTAGA	P	4
*Xho*I	C↓TCGAG	0	6

[a] Only one strand (5′ → 3′) of the DNA sequence recognized by the restriction enzyme is presented.

[b] Amount of enzyme required per microgram of SP01 DNA. Lesser amounts of *Bgl*II and *Hin*fI were not tested. If there was no cleavage or partial cleavage, maximum units per microgram of DNA tested is indicated.

[c] P, Apparent partial cleavage of the DNA.

distinct restriction fragments (Fig. 1). Table 2 shows the approximate sizes of the DNA fragments generated by these enzymes. For each of the three digests, the sum of the sizes of the DNA fragments equaled approximately 140 kilobases (kb), indicating that SP01 DNA has a molecular weight of 0.9×10^8. This agrees with earlier sedimentation velocity studies (13).

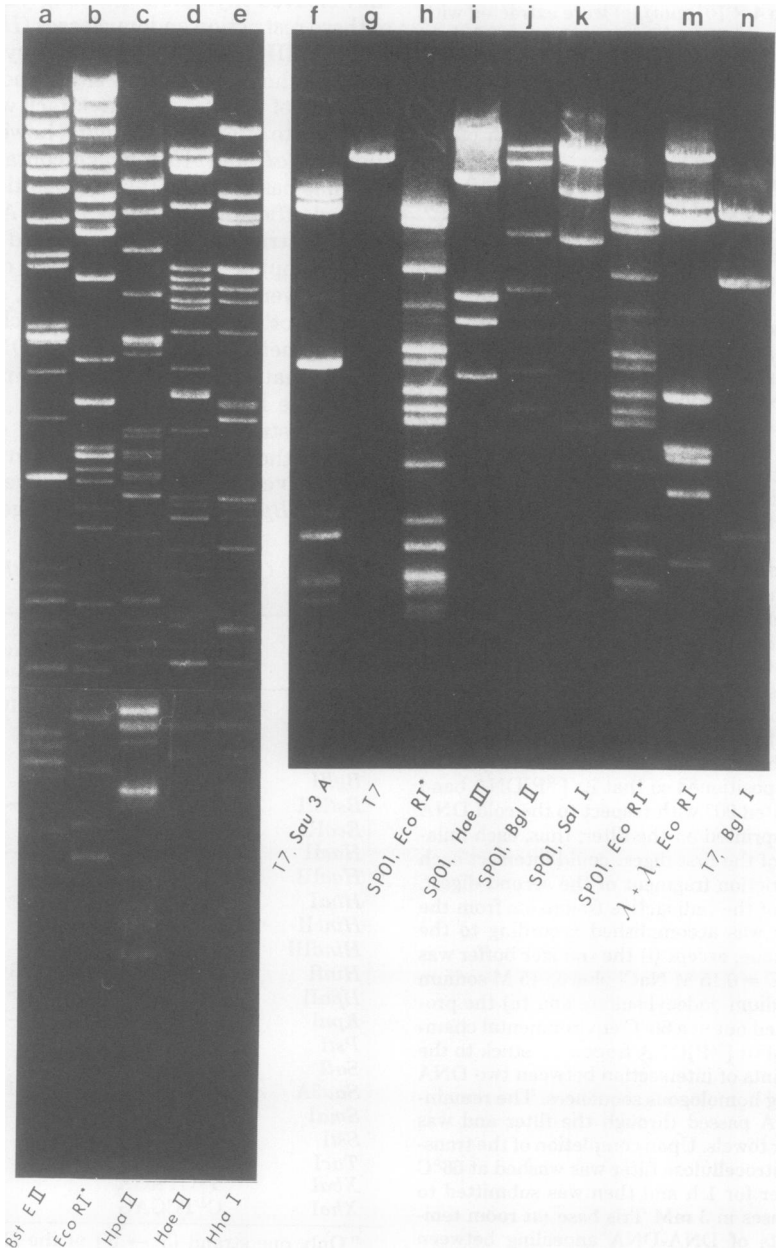

FIG. 1. *Agarose gel electrophoresis of restriction endonuclease digests of SP01 DNA. (a–e) SP01 DNA was cleaved with the indicated restriction enzymes and subjected to electrophoresis on a 1.0% agarose slab gel 30 cm in length. (This is a composite photograph, since the 30-cm gel was too long to be reproduced in a single photograph with our transilluminator.) (f–n) The indicated DNAs were digested with the specified restriction endonucleases and subjected to electrophoresis on a 0.4% agarose slab gel 18 cm in length. As molecular weight markers (see Table 2), uncut T7 DNA (g), Sau3A-cleaved T7 DNA (f), BglI-cleaved T7 DNA (n), and both uncut λ DNA and EcoRI-cleaved λ DNA (m) were subjected to electrophoresis on the 0.4% gel.*

TABLE 2. *Size of SP01 restriction fragments*

Endonuclease(s)	Fragment	
	Designation	Size (kb)[a]
*Eco*RI*	1	21
	2	19.5
	3	14
	4	11.2
	5	10.5
	6	9.2
	7	8.6
	8	7.4
	9	6.8
	10	6.3
	11	5.0
	12	4.0
	13	3.4
	14	3.0
	15	3.0
	16	2.9
	17	2.8
	18	2.5
	19	2.4
	20	2.0
	21	1.8
	22	1.7
	23	1.5
	24	1.4
	25	1.2
	26	1.1
*Hae*III	1	78
	2	29
	3	12
	4	10.4
	5	8.1
	6	2.2
*Sal*I	1	50
	2	40
	3	26
	4	18
	5	6.2
*Hae*III-*Sal*I	a	48
	b	28
	c	26
	d	12
	e	10.4
	f	7.0
	g	4.3
	h	2.2
	i	1.8
	j	0.8
*Bgl*II	1	55
	2	38
	3	19
	4	12.5
	5	8.3
	6	6.8

[a] The sizes of the DNA fragments of less than 40 kb were determined by comparisons of their mobilities on agarose gels with those of λ DNA, *Eco*RI-cut λ DNA (20), T7 DNA, *Sau*3A-cut T7 DNA (12), and *Bgl*I-cut T7 DNA (F. W. Studier, personal communication) (see Fig. 1). The sizes of the fragments over 40 kb were calculated from the sum of the *Eco*RI* fragments contained on each DNA segment.

The restriction endonucleases *Kpn*I, *Eco*RI*, *Bst*EII, and *Hae*II each generated between 15 and 30 distinguishable DNA bands (Fig. 1 and 2); however, several of the DNA bands contained more than one fragment. For example, densitometer tracings of the *Kpn*I digest revealed that *Kpn*I bands 1, 2, and 12 each contained two unresolved fragments, whereas *Kpn*I band 7 appeared to contain three unresolved fragments (Fig. 2). The digests produced by *Hpa*II and *Hha*I were even more complicated and contained more than 40 discernible fragments (Fig. 1), whereas *Alu*I, *Hinf*I and *Sau*3A each di-

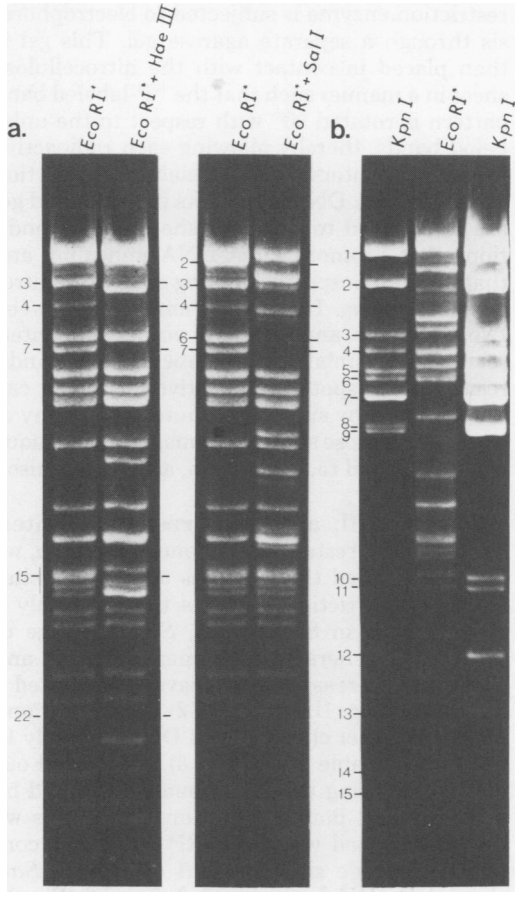

FIG. 2. *Agarose gel electrophoresis of double digestion of SP01 DNA with two restriction endonucleases. (a) An EcoRI* digest of SP01 DNA was cleaved with HaeIII or SalI and subjected to electrophoresis on a 0.7% agarose slab gel. The original EcoRI* digest was compared with the double digest; the numbers indicate EcoRI* fragments that were cleaved by HaeIII or SalI. (b) SP01 DNA was digested with KpnI and subjected to electrophoresis. To visualize small fragments, two different amounts, 0.7 (left lane) and 2.0 (right lane) μg, of KpnI-cleaved DNA were subjected to electrophoresis. All bands generated by KpnI are numbered.*

gested SP01 DNA into more than 100 small fragments, the largest being about 1.5, 1.8, and 2.3 kb, respectively (data not shown).

Ordering restriction fragments. For mapping restriction fragments we used a two-dimensional DNA-DNA annealing technique described by Clyde Hutchison III (personal communication; see reference 16). First, an unlabeled restriction digest of the DNA is layered across the top of an agarose slab gel and subjected to electrophoresis. The separated restriction fragments are transferred to a nitrocellulose sheet by the blotting technique of Southern (17). Second, a [^{32}P]DNA digest generated by a different restriction enzyme is subjected to electrophoresis through a separate agarose gel. This gel is then placed in contact with the nitrocellulose sheet in a manner such that the ^{32}P-labeled band pattern is rotated 90° with respect to the unlabeled bands, thereby allowing each radioactive fragment to intersect each unlabeled restriction fragment. The DNA fragments in the second gel are transferred to the filter sheet under conditions that promote DNA-DNA annealing and that inhibit nonspecific binding of DNA to nitrocellulose filters. If there is homology between two fragments, annealing will occur at the intersection of the unlabeled and labeled DNA bands, resulting in a spot of radioactive DNA that can be visualized by subsequent autoradiography of the nitrocellulose sheet. This mapping technique will be referred to, henceforth, as the Hutchison procedure.

***Sal*I, *Hae*III, and *Bgl*II restriction sites.** To provide a restriction endonuclease map, we first determined the locations of cleavage sites for those restriction enzymes that had only a few cut sites in SP01 DNA. *Sal*I cleavage of SP01 DNA generated 5 fragments (Fig. 1k and Table 2), whereas *Hae*III cleavage generated 6 fragments (Fig. 1i and Table 2). Since *Sal*I and *Hae*III together cleaved SP01 DNA into only 10 fragments (Table 2 and Fig. 3), we started our map by ordering those fragments generated by a *Hae*III-*Sal*I double digestion. To do this we first determined which *Eco*RI* fragments contained cleavage sites for *Sal*I or *Hae*III. *Sal*I cleaved *Eco*RI* fragments 2, 3, 6 and 7 (Fig. 2). (It also cleaved fragment 4, which contained fragment 7 [see below and Fig. 8].) Only 4 *Eco*RI* fragments (fragments 3, 7 [and 4], 15, and 22) were cleaved by *Hae*III, even though this enzyme had five cut sites on SP01 DNA. However, since *Eco*RI* fragment 15 was present in greater-than-stoichiometric amounts, we suspected that fragment 15 was present at two different locations on the phage genome (an assumption verified below) and hence accounted for two cleavage sites.

Second, we utilized the Hutchison procedure to find which *Hae*III-*Sal*I fragments annealed to each of the six *Eco*RI* fragments (fragments 2, 3, 6, 7, 15, and 22) cleaved in a *Hae*III-*Sal*I double digest. Since both *Sal*I and *Hae*III cleaved *Eco*RI* fragments 3 and 7 (Fig. 2), we expected the *Hae*III-*Sal*I double digest to contain one restriction fragment that annealed only to *Eco*RI* fragment 3 and another that annealed only to *Eco*RI* fragment 7; these turned out to be the two smallest *Hae*III-*Sal*I fragments, namely, i and j, respectively (Table 3 and Fig. 3). Furthermore, the Hutchison autoradiograph of Fig. 3 showed that *Hae*III-*Sal*I fragments b and g also overlapped *Eco*RI* fragment 3, producing the map order b-i-g, and that *Hae*III-*Sal*I fragments d and f overlapped *Eco*RI* fragment 7, giving the order d-j-f. In addition, *Hae*III-*Sal*I fragments b and d had to be adjacent, as both contained sequences present on *Eco*RI* fragment 22, and *Hae*III-*Sal*I fragments c and g had be adjacent, as both contained sequences present on *Eco*RI* fragment 6 (Fig. 3 and Table 3). From these data, *Hae*III-*Sal*I fragments b, c, d, f, g, h, and i could be ordered c-g-i-b-d-j-f (see Fig. 8).

As predicted above, the Hutchison autoradiograph of Fig. 3 showed that four different *Hae*III-*Sal*I segments, fragments a, e, f, and h, annealed with *Eco*RI* fragment 15. Therefore, it was not possible to determine directly which pairs of *Hae*III-*Sal*I fragments were adjacent. However, since *Eco*RI* fragment 15 was cleaved by *Hae*III and not by *Sal*I, *Hae*III-*Sal*I fragment f (which is located at the right end of the above sequence) and *Hae*III-*Sal*I fragment a, e, or h must be contained on one of the five *Sal*I fragments. By comparing the sizes of the above four *Hae*III-*Sal*I fragments and the *Sal*I fragments (Table 2), and the *Eco*RI* fragments with which the *Hae*III-*Sal*I and *Sal*I fragments annealed (Table 3), we could show in the following manner that *Hae*III-*Sal*I fragments f plus e corresponded to *Sal*I fragment 4. *Sal*I fragment 4 was 18 kb and contained sequences present on at least *Eco*RI* fragments 4, 10, 15, 20, and 26 (Table 3); *Hae-Sal*I fragment e was the only *Hae*III-*Sal*I fragment of less than 18 kb that annealed with *Eco*RI* fragments 10, 15, and 26. *Hae*III-*Sal*I fragments f and h also contained sequences in common with the rest of the *Eco*RI* sequences present on *Sal*I fragment 4; however, the size of fragments e plus h (10.4 + 2.2 kb) was not close to the size of *Sal*I fragment 4 (18 kb), whereas the size of fragments e plus f (10.4 + 7 kb) was in good agreement.

If *Hae*III-*Sal*I fragments e and f were adjacent, it followed, then, that the other pair of *Hae*III-*Sal*I fragments (a and h) that annealed

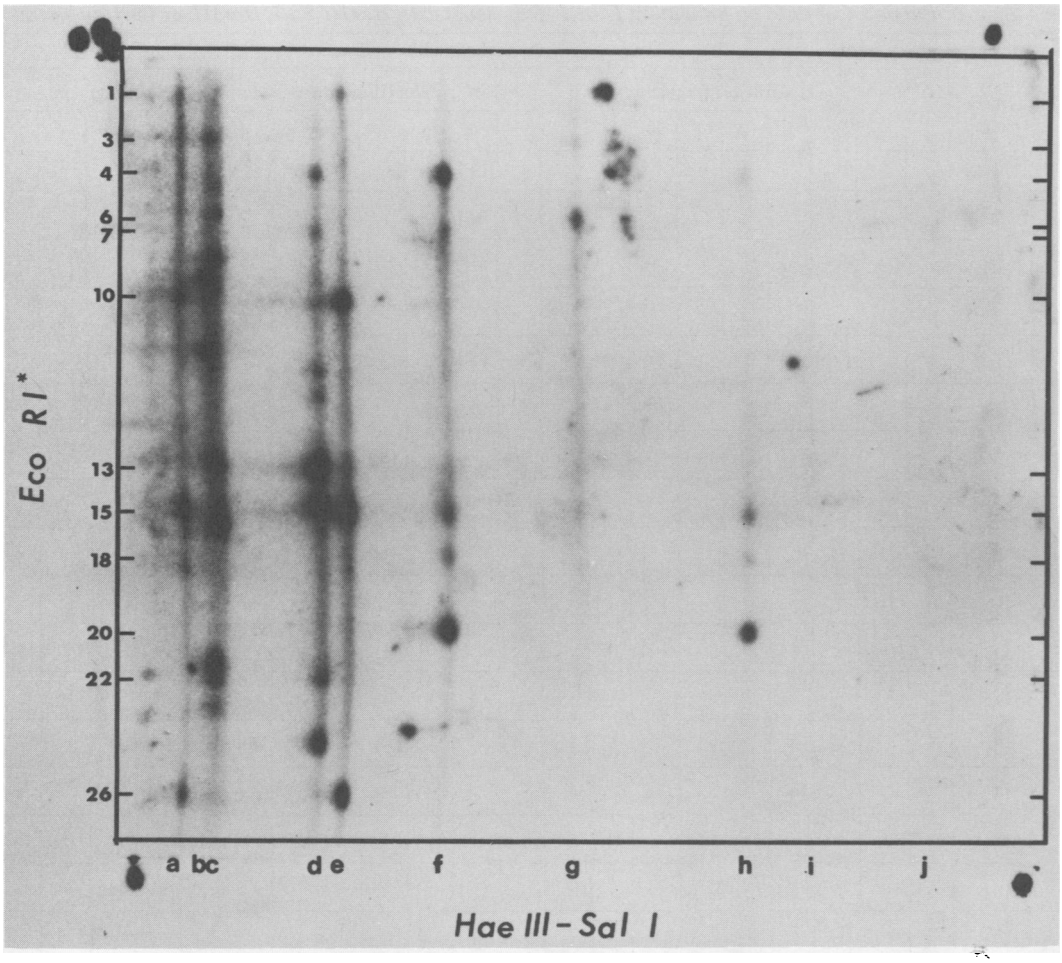

FIG. 3. *Autoradiograph of an EcoRI* digest annealed with a HaeIII-SalI double digest. The positions of separated fragments from an unlabeled HaeIII-SalI digest (12 μg) are indicated by the letters a through j along the abscissa and can be seen as lines in the autoradiograph. The positions of certain of the separated fragments from an EcoRI* digest (6 μg; 8 × 10⁶ cpm) of in vivo-labeled SP01 [^{32}P]DNA are indicated along the ordinate. Dark spots at the intersections of bands result from annealing of ^{32}P-labeled EcoRI* fragments to HaeIII-SalI fragments. The data from the original autoradiograph of this figure are summarized in Table 3. (Since the restriction enzyme EcoRI* does not yield a limit digest, annealing to small amounts of "EcoRI" fragments which result from incomplete digestion is sometimes observed. In particular, the two spots located between EcoRI* fragments 11 and 12 on HaeIII-SalI fragment d represent such a case.)*

with *Eco*RI* fragment 15 were contiguous. (In fact, in a manner similar to that just outlined, we could show that *Hae*III-*Sal*I fragments a plus h [48 + 2.2 kb] corresponded to *Sal*I fragment 1 [50 kb].) Combining these data with those above, we deduced the order c-g-i-b-d-j-f-e. This left unmapped the adjacent pair of *Hae*III-*Sal*I fragments a and h, which had to be located at one end of the SP01 genome. (In principle, we should have been able to order this pair of fragments as *Hae*III-*Sal*I fragment a or h, and *Hae*III-*Sal*I fragment c or e should have annealed to *Eco*RI* fragment 2, the only remaining *Eco*RI* fragment cleaved by *Hae*III or *Sal*I that had not been accounted for in our map. However, *Eco*RI* fragment 2 did not anneal well with any of the *Hae*III-*Sal*I fragments, so it was not possible to determine from the Hutchison autoradiograph alone at which end *Hae*III-*Sal*I fragments a plus h mapped. We have frequently observed poor DNA-DNA annealing between two very large restriction fragments, probably as a result of inefficient transfer of the large DNA fragments from the gels [17].)

We were, however, able to determine at which end of the phage genome *Hae*III- *Sal*I fragments

TABLE 3. *Summary of data on annealing EcoRI* fragments with HaeIII-SalI, HaeIII, or SalI fragments*

*Eco*RI* fragment	Annealing[a] with:																				
	*Hae*III-*Sal*I fragment:										*Hae*III fragment:						*Sal*I fragment:				
	a	b	c	d	e	f	g	h	i	j	1	2	3	4	5	6	1	2	3	4	5
1					+						(+)			+							
2											(+)										
3		+					(+)		(+)			+					*				+
4				+		+		(+)		(+)			+		+	+	+	+		+	
5			(+)								(+)								(+)		
6			(+)				+				(+)						*		+		+
7				(+)		(+)				(+)			(+)		(+)		*	(+)			
8			(+)								(+)								(+)		
9		+										+					*	(+)			
10	+				+						+			+			+			+	
11		+										+					*	(+)			
12											(+)						(+)				
13			+	+									+				*	+	+		
14				+									+				*	+			
15	+				+	+		+			+			+	(+)	(+)	+			+	
16			+								(+)								+		
17			+								(+)								+		
18						+		(+)							+	+	+			(+)	
19	(+)										(+)						+				
20						+		+							+	+	+			+	
21		+										+					*	+			
22		+		+								+	(+)				*	+			
23		(+)										(+)					*	+			
24				+									(+)				*	+			
25																	(+)				
26	+				+						+			+			+			+	

[a] Symbols: +, dark spot on autoradiograph depicting annealing between indicated fragments (see Fig. 3); (+), light spot; *, light spot believed to come from annealing of the *Eco*RI* fragment to a small amount of a 46-kb *Sal*I fragment which was not resolved from *Sal*I fragment 1 (this 46-kb fragment resulted from incomplete cleavage between *Sal*I fragments 2 and 5).

a plus h were located in the following manner. First, we sought to determine which *Hae*III fragment contained these *Hae*III-*Sal*I fragments. Since *Hae*III-*Sal*I fragment a was so large (48 kb), only *Hae*III fragment 1 (78 kb) was large enough to contain it. Therefore, to map the

location of the adjacent pair of *Hae*III-*Sal*I fragments a plus h, we merely had to determine from which end of the genome *Hae*III fragment 1 was derived. *Hae*III fragment 1 contained sequences in common with *Hae*III-*Sal*I fragments c and g (located at the left of our map) in addition to *Hae*III-*Sal*I fragment a (Table 3). Therefore, *Hae*III fragment 1 was located at the left end of our map, and the order of the *Hae*III-*Sal*I fragments contained on this fragment had to be a-c-g (see above). Moreover, since *Hae*III-*Sal*I fragment h was a separate *Hae*III fragment (fragment 6; see Table 2) and was adjacent to *Hae*III-*Sal*I fragment a, it had to be located at the left end of our map, and the order of the *Hae*III-*Sal*I fragments became h-a-c-g-i-b-d-j-f-e (see Fig. 8).

By comparing the sizes of the *Hae*III, *Sal*I, and *Hae*III-*Sal*I fragments (Table 2) and the *Eco*RI* fragments with which they annealed (Table 3), we could show that *Hae*III-*Sal*I fragments h plus a corresponded to *Sal*I fragment 1, that fragment c corresponded to *Sal*I fragment 3, that fragments a plus c corresponded to *Sal*I fragment 5, that fragments b plus d plus j corresponded to *Sal*I fragment 2, and that e plus f fragments corresponded to *Sal*I fragment 4. Therefore, the order of the *Sal*I fragments had to be 1-3-5-2-4 (see Fig. 8). Similarly, it could be shown that *Hae*III-*Sal*I fragment h corresponded to *Hae*III fragment 6, that fragments a plus c plus g corresponded to *Hae*III fragment 1, that fragments b plus i corresponded to *Hae*III fragment 2, that fragment d corresponded to *Hae*III fragment 3, that fragments f plus j corresponded to *Hae*III fragment 5, and that fragment c corresponded to *Hae*III fragment 4. Thus, the order of the *Hae*III fragments had to be 6-1-2-3-5-4 (see Fig. 8). (A simple analysis of the data presented in Table 3 directly confirmed much of this map order. For example, *Hae*III fragments 5 and 3 and *Hae*III fragments 2 and 3 overlapped *Eco*RI* fragments 7 and 22, respectively. Thus, these *Hae*III fragments had to be in the order 2-3-5.)

*Bgl*II cleaved SP01 DNA five times, to produce six restriction fragments (Fig. 1j and Table 2). *Bgl*II cleavage sites occurred in *Eco*RI* fragments 1, 3, 6, 8, and 13b (data not shown). The same procedures described above to construct the *Hae*III-*Sal*I restriction map were used to derive the *Bgl*II map shown in Figure 8. *Bgl*II-*Sal*I (see Fig. 7) and *Bgl*II-*Hae*III double digests were used to confirm this map order.

_Eco_RI* restriction fragments. When SP01 DNA was digested with the restriction endonuclease *Eco*RI under normal assay conditions, incomplete cleavage resulted even if excess amounts of enzyme were used (1, 8, 18). However, when reaction conditions of high pH and low salt were used, a more complete cleavage pattern was observed (18; Fig. 1). These conditions reportedly reduce the recognition specificity of *Eco*RI (5'GAATTC3') to the altered endonucleolytic activity *Eco*RI* (5'AATT3') (15), although it is not clear that this happens in the 5-hydroxymethyluracil-containing SP01 DNA (1). As analyzed by agarose gel electrophoresis, *Eco*RI* digestion of SP01 DNA yielded 26 visible fragments (18; Fig. 1 and 2). As reported previously (18), several fragments (fragments 5, 7, and 18) were clearly present in less-than-stoichiometric amounts. Densitometer tracings also revealed greater-than-stoichiometric amounts of fragments 13, 15, and 26.

To determine which fragments contained sequences in common, either as a result of incomplete cleavage of the DNA or due to redundancies in the genome, we annealed an *Eco*RI* digest of SP01 DNA with itself by the Hutchison procedure. Fragment 4 contained sequences in common with fragments 7 and 18, whereas fragment 5 shared sequences with fragments 8 and 17 (Fig. 4). Prolonged digestion of SP01 DNA led to an increase in the amounts of *Eco*RI* fragments 7 and 18 concurrent with a decrease in the quantity of fragment 4; also, the sum of the molecular weights of fragments 7 and 18 approximately equaled the molecular weight of fragment 4 (Table 2). Thus, *Eco*RI* fragment 4 had to be a partial digestion product composed of *Eco*RI* fragments 7 and 18. Similar arguments were used to conclude that *Eco*RI* fragment 5 was a partial digestion product composed of *Eco*RI* fragments 8 and 17. Close examination of the autoradiographs in Fig. 4 also revealed the presence of another partial digestion product, just above fragment 10, that we have called 10'. Fragment 10' was composed of fragments 13b and 17 (Fig. 4). In addition, extensive digestion cleaved *Eco*RI* fragment 3 into fragment 8' (about the size of fragment 8) and fragment 10'' (about the size of fragment 10) (see Fig. 4 and 8).

Besides the fragments which shared common sequences as a result of incomplete cleavage at certain restriction sites, fragments 1 and 10 and also fragments 18 and 20 contained common sequences which could not be explained by partial digestion. For example, fragment 20, which is smaller than fragment 18, appeared before fragment 18 during the course of digestion. These homologies must, therefore, have resulted from repeated sequences in the DNA. In fact, as will be documented below, phage SP01 is terminally redundant, and fragments 18 and 10 map at one end of the genome, whereas fragments 20 and 1 map at the other end (2).

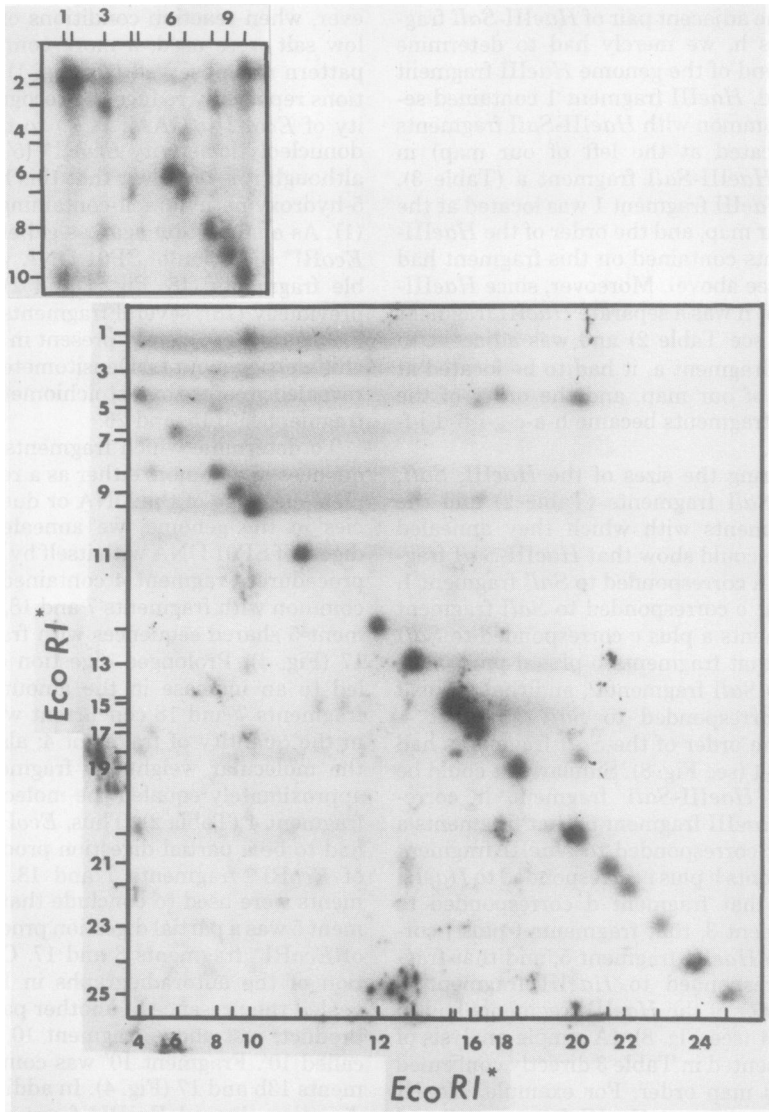

FIG. 4. *DNA-DNA annealing of EcoRI* fragments by the Hutchison procedure. Since the largest ^{32}P-labeled EcoRI* fragments are not shown in the large autoradiograph, a second, small autoradiograph is included to show the region containing EcoRI* fragments 1 through 10. The positions of separated fragments from an unlabeled EcoRI* digest (20 μg) are indicated by the numbers 1 through 25 along the ordinate of the large autoradiograph. The positions of ^{32}P-labeled EcoRI* fragments (6 μg, 7.5 × 10^6 cpm) are indicated on the abscissa.*

SP01 DNA is terminally redundant. During the course of mapping the *Hae*III, *Sal*I, and *Bgl*II sites on the phage genome, it became apparent that several *Eco*RI* fragments contained sequences that were present at both the left and the right ends of SP01 DNA. Each of these fragments (*Eco*RI* fragments 1, 10, 15, 18, 20, and 26) annealed with *Hae*III-*Sal*I fragments h and a, at the left end of our map, and with *Hae*III-*Sal*I fragments f and e, at the right end (see Fig. 3 and 8). This demonstrated that SP01 DNA was terminally redundant, in agreement with the genetic studies of Cregg and Stewart (2).

What was the structure of this terminal repetition? Two of these *Eco*RI* fragments (15 and 26) were present in two copies per genome and had to be contained entirely within the terminal repetition. The other *Eco*RI* fragments in the terminally redundant region (1, 10, 18, and 20) were present only once per genome; these DNAs presumably represented either overlaps between

repeated and nonrepeated sequences or restriction fragments from the termini of SP01 DNA.

To establish the structure of the terminal repetition, we determined which of the single-copy *Eco*RI* fragments were actually located at each end of our restriction map. *Eco*RI* fragments 18 and 20 both annealed with *Hae*III-*Sal*I fragment h, located at the left end of our map, and with *Hae*III-*Sal*I fragment f, located near the right end of the map (see Fig. 3 and 8). Since *Eco*RI* fragments 18 and 7 arose from cleavage of *Eco*RI* fragment 4, as discussed above, and since part of *Eco*RI* fragment 7 was located on *Hae*III-*Sal*I fragment f (Fig. 3), *Eco*RI* fragment 18 must also have been located on *Hae*III-*Sal*I fragment f. Therefore, *Eco*RI* fragment 20 had to be located on *Hae*III-*Sal*I fragment h. The following reasoning confirmed these assigned locations. Neither *Eco*RI* fragment 18 nor *Eco*RI* fragment 20 was cleaved by *Hae*III or *Sal*I (Fig. 2), indicating that each had to be contained on a single *Hae*III-*Sal*I restriction fragment. Since *Hae*III-*Sal*I fragment h (2.2 kb) was too small to contain *Eco*RI* fragment 18 (2.4 kb), it had to contain *Eco*RI* fragment 20 (2.0 kb) instead. Thus, *Eco*RI* fragment 20 was located at the left end of our physical map and contained sequences that were repeated in *Eco*RI* fragment 18, which was near the right end.

*Eco*RI* fragments 1 and 10 each annealed with both *Hae*III-*Sal*I fragment a (located near the left end of the map) and *Hae*III-*Sal*I fragment e (located at the right end of the map) (see Fig. 3 and 8). Since neither *Hae*III nor *Sal*I cleaved *Eco*RI* fragment 1 (21 kb) (Fig. 2) and since *Hae*III-*Sal*I fragment e was only 10.4 kb in size, the sequences on *Eco*RI* fragment 1 had to be located on *Hae*III-*Sal*I fragment a (48 kb), near the left end of the map. *Eco*RI* fragment 10 (6.3 kb), hence, had to be present at the right end, on *Hae*III-*Sal*I fragment e.

Having established that *Eco*RI* fragments 20 and 1 were located at the left end of our map and that *Eco*RI* fragments 18 and 10 were at the right end, it was only necessary to order those *Eco*RI* fragments that annealed to *Hae*III-*Sal*I fragments f plus e and h plus a to complete the structure of the terminal redundancy. *Hae*III-*Sal*I fragment f annealed *Eco*RI* fragments 7 (and 4) and 15 as well as *Eco*RI* fragments 18 and 20 (Fig. 3). As discussed earlier, *Eco*RI* fragments 7 (and 4) and 15 were cleaved by *Sal*I and *Hae*III, respectively (Fig. 2), and overlapped the left and right borders of *Hae*III-*Sal*I fragment f. In addition, *Eco*RI* fragment 18 was shown to be adjacent to *Eco*RI* fragment 7 (Fig. 4); therefore, the fragment order had to be 7-18-15.

Now we had to order the *Eco*RI* fragments that annealed with *Hae*III-*Sal*I fragment e, namely, fragments 10, 15, and 26. Annealing of an *Eco*RI* digest with an "*Eco*RI" digest (a partial *Eco*RI* digest) indicated that there was an *Eco*RI fragment (fragment k) of about 4.2 kb containing *Eco*RI* fragments 15 and 26 (Fig. 5). This placed *Eco*RI* fragment 26 next to fragment 15. Since *Eco*RI* fragment 15 overlapped the left border of *Hae*III-*Sal*I fragment e and since *Eco*RI* fragment 26 was adjacent to fragment 15, to give the order 15-26, then *Eco*RI* fragment 10, the only remaining fragment which contained sequences on *Hae*III-*Sal*I fragment e, had to be at the rightmost end of the map to give the order 15-26-10. Combining this order with that of *Eco*RI* fragments having sequences on *Hae*III-*Sal*I fragment f, the final order for what we have designated as the right end of the physical map became 7-18-15-26-10 (see Fig. 8).

Sequences present from within *Eco*RI* fragment 18 through fragment 10 were repeated at the left end of the map in the *Eco*RI* fragments 20-15-26-1. This arrangement was confirmed by annealing an *Eco*RI* digest with a *Bgl*II digest, *Bgl*II fragment 3, located at the left end of the physical map, annealed *Eco*RI* fragments 1, 4, 10, 15, 18, 20, and 26 (data not shown). Redundant sequences accounted for annealing to *Eco*RI* fragments 4, 10, and 18, which were actually located at the right end of the map. This placed fragments 1, 15, 20, and 26 at the left end. *Hae*III-*Sal*I fragment h annealed *Eco*RI* fragments 20 and 15. Since *Eco*RI* fragment 15 was cleaved by *Hae*III, the order had to be 20-15-. For the reasons discussed above, we knew that *Eco*RI* fragment 26 was adjacent to fragment 15, to give the order 20-15-26-. This placed *Eco*RI* fragment 1, the only remaining *Eco*RI* fragment with sequences on *Bgl*II fragment 3, adjacent to *Eco*RI* fragment 26.

The orders of the *Eco*RI* fragments at the left and right ends of our physical map were, then, 20-15-26-1- and -18-15-26-10, respectively. Since the sequences contained within *Eco*RI* fragment 20 were repeated within fragment 18 and those within fragment 10 were repeated within fragment 1, the size of the terminally redundant ends of SP01 DNA equals the sum of the sizes of *Eco*RI* restriction fragments 20, 15, 26, and 10, or 12.4 kb.

Mapping *Eco*RI* restriction sites. To map the *Eco*RI* fragments, we used the Hutchison procedure to order groups of *Eco*RI* DNAs on *Hae*III-*Sal*I fragments. This grouping is discussed in the order of the *Hae*III-*Sal*I fragments: h-a-c-g-i-b-d-j-f-e (see Fig. 8). As discussed above, *Hae*III-*Sal*I fragments h plus a contained

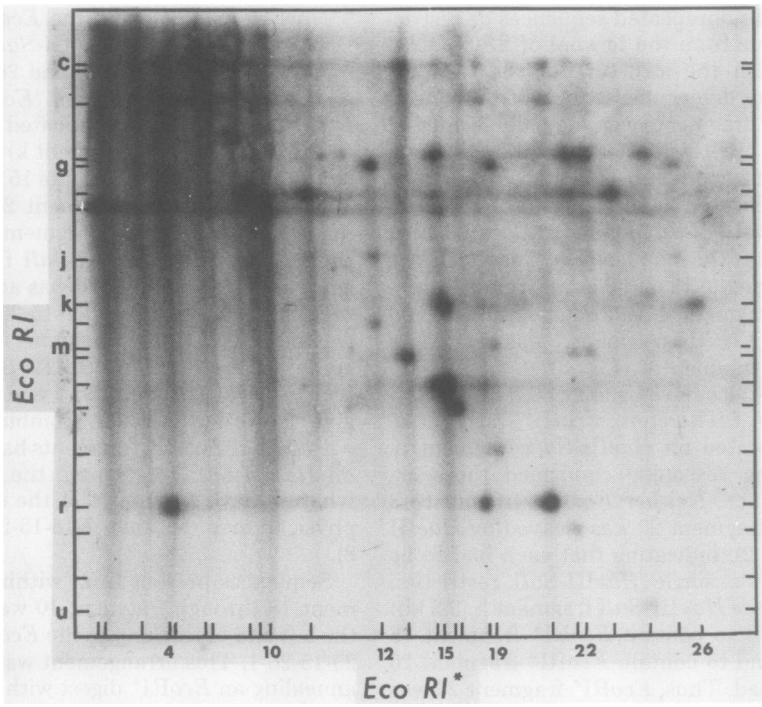

FIG. 5. *Autoradiograph of an "EcoRI" digest annealed to an EcoRI* digest. The unlabeled EcoRI* fragments (22 μg) are numbered along the abscissa and can be seen as shaded lines in the autoradiograph. The positions of the ^{32}P-labeled "EcoRI" fragments (4 μg; 8 × 10^6 cpm) are indicated by the letters along the ordinate.*

the terminal repetition consisting of *Eco*RI* fragments 20-15-26-1. However, poor annealing of the *Eco*RI* digests to the large *Hae*III-*Sal*I fragment a made it difficult to decipher directly all of the other *Eco*RI* fragments contained on this DNA (see below). *Eco*RI* fragments 5, 6, 8, 13b, 16, and 17 were located on the next *Hae*III-*Sal*I fragment, fragment c, and *Hae*III-*Sal*I fragment g contained sequences from *Eco*RI* fragments 3 and 6 (Fig. 3). *Hae*III-*Sal*I fragment i simply had a small part of *Eco*RI* fragment 3, and *Hae*III-*Sal*I fragment b contained *Eco*RI* fragments 3, 9, 11, 21, and 22. Fragment d contained sequences from *Eco*RI* fragments 7, 13a, 14, 22, and 24 (Fig. 3). Finally, *Hae*III-*Sal*I fragment j had a small piece of *Eco*RI* fragment 7, and fragments f plus e contained the remainder of *Eco*RI* fragment 7 and the terminal repetition consisting of *Eco*RI* fragments 18-15-26-10 (Fig. 3). Next, we determined the exact order of *Eco*RI* fragments within each of the above groups as described below.

Ordering the *Eco*RI* fragments (7, 13a, 14, 22, and 24) on *Hae*III-*Sal*I fragment d. *Eco*RI* fragments 7 and 22 each contained a *Hae*III cleavage site (Fig. 2) and were therefore located at the ends of *Hae*III-*Sal*I fragment d. This meant that *Eco*RI* fragments 13a, 14, and 24 were located internally. Using the Hutchison procedure, we identified a *Kpn*I fragment (fragment 8) that annealed to *Eco*RI* fragments 21, 22, and 14 (Fig. 6). Since only *Eco*RI* fragments 14 and 22 had sequences in common with *Hae*III-*Sal*I fragment d, *Eco*RI* fragment 14 had to be adjacent to fragment 22. (As *Eco*RI* fragment 21 must also have been adjacent to fragment 22, the order became 21-22-14.) Furthermore, we identified an 8-kb "*Eco*RI" fragment (f) composed of *Eco*RI* fragments 14, 21, 22, and 24 (Fig. 5). Since *Eco*RI* fragment 24 also had sequences in common with *Hae*III-*Sal*I fragment d, the order of *Eco*RI* fragments had to be 21-22-14-24. Similarly, we identified a 14-kb "*Eco*RI" DNA segment (fragment c) containing *Eco*RI* fragments 7, 13a, and 18 (Fig. 5). Since *Eco*RI* fragment 18 was next to fragment 7 (discussed above) and not included on *Hae*III-*Sal*I fragment d, *Eco*RI* fragment 13a, which was located on fragment d, had to be adjacent to *Eco*RI* fragment 7, giving the order 13a-7-18. Thus, the order of *Eco*RI* fragments with sequences contained on *Hae*III-*Sal*I fragment d was 22-14-24-13a-7 (see Fig. 8).

Ordering the *Eco*RI* fragments (3, 9, 11,

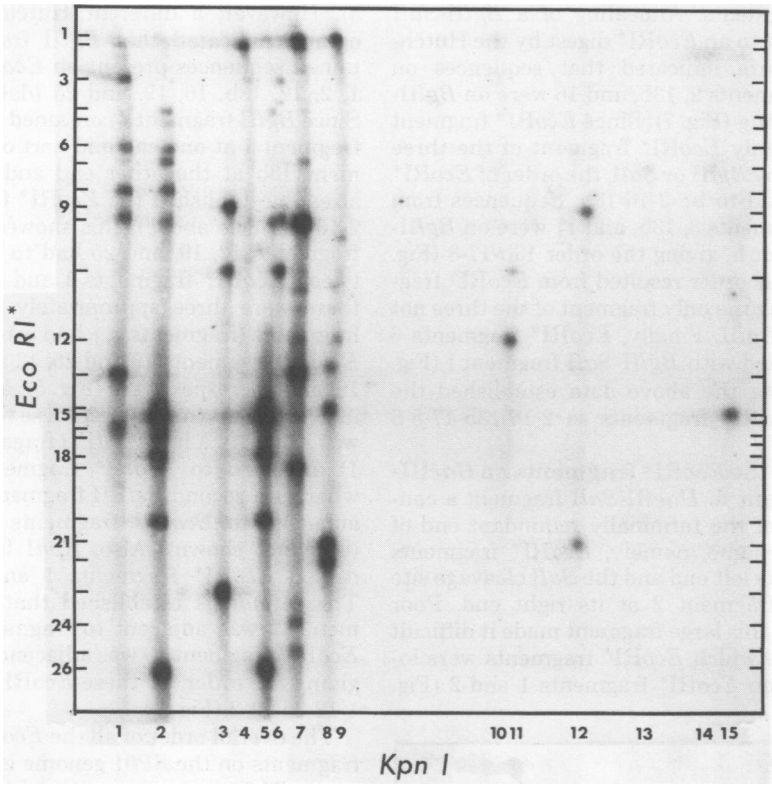

FIG. 6. *Autoradiograph of a KpnI digest annealed to an EcoRI* digest. The unlabeled KpnI fragments (21 μg) are numbered along the abscissa and can be seen as shaded lines in the autoradiograph. KpnI bands 1, 2, and 12 each contained two unresolved fragments, whereas KpnI band 7 apparently consisted of three unresolved fragments. The positions of the ^{32}P-labeled EcoRI* fragments (1.5 μg; 1.8 × 10^6 cpm) are indicated by the numbers along the ordinate. A dark spot indicates the annealing of a ^{32}P-labeled EcoRI* fragment to a KpnI fragment. Whereas all the data presented in this figure are consistent with the EcoRI* restriction map of Fig. 8, only annealing to KpnI fragments 3, 6, 9, and 12 is discussed in the text. KpnI fragment 3 annealed EcoRI* fragments 9, 11, and 23; KpnI fragment 6 annealed EcoRI* fragments 3, 10", and 11; and KpnI fragment 9 annealed EcoRI* fragments 1 and 12. (The adjacent KpnI fragment [fragment 8] annealed EcoRI* fragments 14, 21, and 22. The spot just above EcoRI* fragment 13 resulted from annealing of KpnI fragment 8 to an "EcoRI" fragment composed of EcoRI* fragments 21 and 22. Additional faint spots which are not located at the intersections of KpnI fragment 8 or 9 with EcoRI* fragments [for example, below EcoRI* fragment 10 and between EcoRI* fragments 11 and 12] also resulted from annealing to minor amounts of "EcoRI" fragments present in the EcoRI* digest [see legend to Fig. 3].)*

21, 22, and 23) on *Hae*III-*Sal*I fragment b. *Eco*RI* fragments 3 and 22, which contained *Sal*I and *Hae*III cleavage sites, respectively, were located at the ends of *Hae*III-*Sal*I fragment b; therefore, *Eco*RI* fragments 9, 11, 21, and 23 must have been located internally (Fig. 3). As discussed above, *Eco*RI* fragment 21 was adjacent to fragment 22. The results of annealing with *Kpn*I fragment 12 indicated that *Eco*RI* fragment 9 was adjacent to fragment 21, whereas annealing with *Kpn*I fragment 6 indicated that *Eco*RI* fragment 11 was adjacent to fragment 3 (Fig. 6). Finally, *Kpn*I fragment 3 contained sequences present on *Eco*RI* fragments 9, 11, and 23 (Fig. 6). We therefore concluded that the order of *Eco*RI* fragments was 3-11-23-9-21-22 (see Fig. 8). This order was confirmed by the existence of two *Bst*EII fragments: one that contained sequences from *Eco*RI* fragments 3, 11, and 23 and another with sequences from *Eco*RI* fragments 9, 21, and 22 (data not shown).

Ordering the *Eco*RI* fragments (2, 6, 8, 13b, 16, and 17) on *Hae*III-*Sal*I fragment c. *Eco*RI* fragments 6 and 2, which were both cleaved by *Sal*I (Fig. 2), were located at the ends of *Hae*III-*Sal*I fragment c; therefore, *Eco*RI* fragments 8, 13b, 16, and 17 had to be located internally (Fig. 3). As *Bgl*II cleaved *Eco*RI* fragments 6, 8, and 13b, this restriction enzyme was particularly useful in ordering the above

*Eco*RI* fragments. Annealing of a *Bgl*II-*Sal*I double digest to an *Eco*RI* digest by the Hutchison procedure indicated that sequences on *Eco*RI* fragments 2, 13b, and 16 were on *Bgl*II-*Sal*I fragment g (Fig. 7). Since *Eco*RI* fragment 16 was the only *Eco*RI* fragment of the three not cleaved by *Bgl*II or *Sal*I, the order of *Eco*RI* fragments had to be 2-16-13b. Sequences from *Eco*RI* fragments 8, 13b, and 17 were on *Bgl*II-*Sal*I fragment h, giving the order 13b-17-8 (Fig. 7). Again, this order resulted from *Eco*RI* fragment 17 being the only fragment of the three not cleaved by *Bgl*II. Finally, *Eco*RI* fragments 6 and 8 annealed with *Bgl*II-*Sal*I fragment f (Fig. 7). Combining the above data established the order of *Eco*RI* fragments as 2-16-13b-17-8-6 (see Fig. 8).

Ordering the *Eco*RI* fragments on *Hae*III-*Sal*I fragment a. *Hae*III-*Sal*I fragment a contained part of the terminally redundant end of the SP01 genome, namely, *Eco*RI* fragments 15-26-1-, at its left end and the *Sal*I cleavage site in *Eco*RI* fragment 2 at its right end. Poor annealing to this large fragment made it difficult to determine which *Eco*RI* fragments were located between *Eco*RI* fragments 1 and 2 (Fig. 3). However, a different Hutchison autoradiograph indicated that *Bgl*II fragment 2 contained sequences present on *Eco*RI* fragments 1, 2, 12, 13b, 16, 19, and 25 (data not shown). Since *Bgl*II fragment 2 contained part of *Eco*RI* fragment 1 at one end and part of *Eco*RI* fragment 13b at the other end and since we had already established the *Eco*RI* fragment order 2-16-13b (see above), this showed that *Eco*RI* fragments 12, 19, and 25 had to be located between *Eco*RI* fragments 1 and 2. In addition, there were three appropriately sized "*Eco*RI" fragments (fragments g, j, and m) that contained *Eco*RI* fragments 19 and 25, 12 and 25, and 12, 19, and 25, respectively (Fig. 5), a finding which indicated that the order of these three fragments was 12-25-19. A large *Bst*EII fragment (fragment 1) annealed to *Eco*RI* fragments 1 and 12, whereas a second *Bst*EII fragment (fragment 2) annealed to *Eco*RI* fragments 2, 19, and 25 (data not shown). Also, *Kpn*I fragment 9 annealed *Eco*RI* fragments 1 and 12 (Fig. 6). These findings established that *Eco*RI* fragment 12 was adjacent to fragment 1 and that *Eco*RI* fragment 19 was adjacent to fragment 2, giving the order for these *Eco*RI* fragments as 1-12-25-19-2 (Fig. 8).

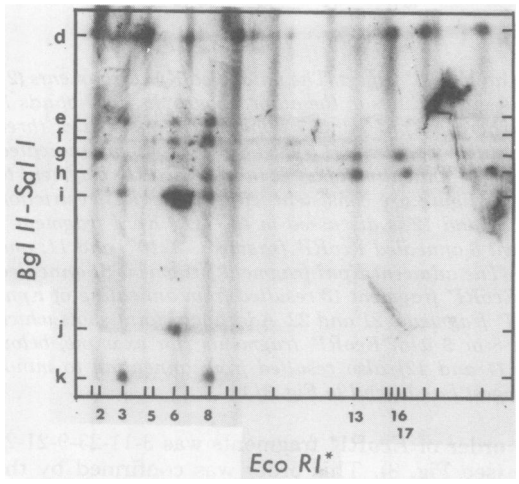

FIG. 7. *Autoradiograph of a BglII-SalI double digest annealed to an EcoRI* digest. The positions of unlabeled EcoRI* fragments 1 through 20 (23 μg) are indicated along the abscissa, whereas the positions of ^{32}P-labeled BglII-SalI fragments d through k (1.4 μg; 5 × 10^6 cpm) are indicated along the ordinate. The map order of the indicated BglII-SalI fragments was g-h-f-j-i-k. BglII-SalI fragment e was composed of fragments i and k and resulted from incomplete SalI cleavage. BglII-SalI fragments e, i, and k annealed to EcoRI* fragment 8' (from EcoRI* fragment 3; see Fig. 8), whereas BglII-SalI fragments f and h annealed to EcoRI* fragment 8 (from EcoRI* fragment 5; see Fig. 8).*

The overall order of all the *Eco*RI* restriction fragments on the SP01 genome is shown in Figure 8. This map was produced by simply integrating the order of the *Eco*RI* fragments on each *Hae*III-*Sal*I fragment with the order of the *Hae*III-*Sal*I fragments themselves. One cautionary note about this map is that it could be missing extremely small *Eco*RI* fragments that might have gone undetected in our gel analysis.

DISCUSSION

Bacteriophage SP01 has a DNA genome of approximately 140 kb (Table 2). Using the Hutchison DNA-DNA annealing procedure, we have mapped the SP01 DNA cleavage sites for the restriction endonucleases *Eco*RI*, *Bgl*II, *Hae*III, and *Sal*I (Fig. 8). The *Eco*RI* restriction map, which divides SP01 DNA into a large number of small segments, is of special interest, since it has allowed us to deduce detailed information about the genetic, physical, and transcriptional organization of the viral genome.

Correlating the physical map of SP01 DNA with the genetic map. SP01 has 36 known cistrons, 34 of which are linked to form a linear map with the cistrons numbered consecutively (14). Cistrons *35* and *36*, the two previously unlinked cistrons, have recently been located at both ends of the genome (2). Cregg and Stewart (1) have used a marker rescue assay to assign 27 of the SP01 cistrons to 10 specific

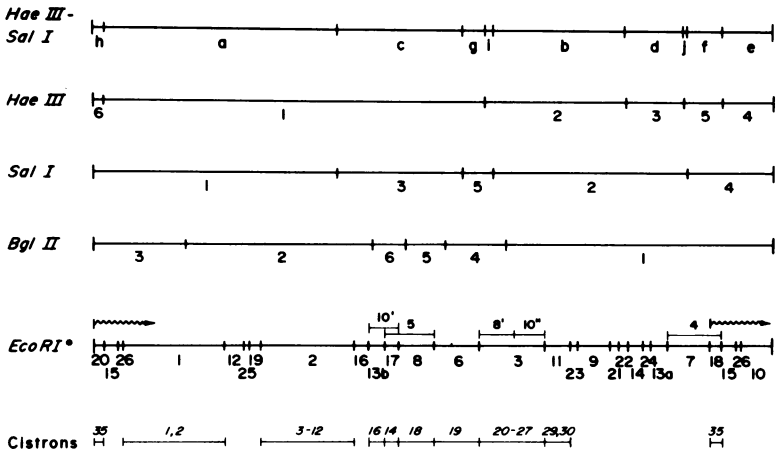

FIG. 8. *Restriction map of SP01 DNA. Fragments are labeled with numbers or letters in order of decreasing molecular weight. The thin lines above the EcoRI* map indicate the positions of fragments that were present in minor amounts (see the text). The wavy arrows above the EcoRI* map denote the regions of terminal redundancy and their orientation. Below the EcoRI* map are the genetic assignments of cistrons to individual fragments as made by Cregg and Stewart (1).*

*Eco*RI* restriction fragments. Since there was a fairly good correlation between our *Eco*RI* fragments and those from Stewart's laboratory (1, 2), we were able to assign cistrons to the *Eco*RI* fragments in our physical map (Fig. 8). With one exception, their genetic data are in excellent agreement with our physical map of the *Eco*RI* restriction fragments. The exception is the position of *Eco*RI* fragment 17; if our *Eco*RI* fragment 17 really contains cistron *14*, it should be located to the left of fragment 13b to agree with the genetic map. However, the DNA-DNA annealing experiment shown in Fig. 7 clearly established that *Eco*RI* fragment 17 is located to the right of fragment 13 b. We cannot at present explain this discrepancy.

Terminal redundancy in SP01 DNA. Okubo et al. (14) were unable to map two of the SP01 cistrons (cistrons *35* and *36*) because mutations in these cistrons showed a high frequency of recombination with all other cistrons. Cregg and Stewart (2) have accounted for this behavior by showing that one of these cistrons is located in a region of terminal redundancy. Their proposal was based on several findings, including the fact that cistron *35* is located on two different restriction fragments (*Eco*RI* fragments 18 and 20) and the fact that one of these fragments (*Eco*RI* fragment 20) is located at the right end of the phage genome. Further evidence for terminal repetition was based on the observation that *Eco*RI* fragments 20 and 10 are absent in *Eco*RI*-cleaved concatemeric DNA of intracellular origin. Since restriction endonuclease cleavage of the concatemeric DNA did not yield new *Eco*RI* fragments, Cregg and Stewart (2) deduced that fragments 10 and 20 must be located at the ends of the genome in a region of terminal redundancy.

Our physical map of the SP01 genome verifies directly the existence of a terminal repetition. In addition, we have shown that the terminal repetition is 12.4 kb in length and consists of *Eco*RI* fragments 20-15-26-1 at the left end of the genome and 18-15-26-10 at the right end. Repeated sequences are joined to nonrepeated DNA at the left end in fragment 1 and at the right end in fragment 18. This terminal redundancy is unusually large; to our knowledge, the largest previously reported terminal repetition is the 10-kb sequence at the ends of phage T5 DNA (7).

Approximate location of early, middle, and late genes on SP01 DNA. In a previous report, we used *Eco*RI* restriction fragments of SP01 DNA as specific hybridization probes to examine the temporal program of phage transcription (18). Cells of *B. subtilis* were pulse-labeled at various times after infection by wild-type SP01 or by a mutant in regulatory gene *28*, the gene whose product is required for middle RNA synthesis, or by mutants in regulatory genes *33* or *34*, the genes whose products are needed for late gene transcription (17). Radioactive RNA from the pulse-labeled bacteria was then hybridized to electrophoretically separated *Eco*RI* restriction fragments of SP01 DNA. From the pattern of hybridization, we identified DNA fragments that contained early, middle, or late phage genes. By combining this information with the map order of the *Eco*RI* fragments, we have determined which regions of the genome are actively transcribed at early, middle, or late

times during the lytic cycle. In Fig. 9, the *Eco*RI* fragments are represented along the abscissa, and the thick, thin, and dotted lines represent the relative amounts of early, middle, or late labeled RNAs that hybridized to each fragment. These lines were taken from the data of Talkington and Pero (18), and the relative amounts of hybridization have not been normalized to the lengths of the individual DNAs.

Although the hybridization data are only semiquantitative, a striking result clearly emerges from this analysis. RNA that is synthesized at the earliest stage of the lytic cycle is copied predominantly from the terminally redundant ends of the genome. Thus, there are two copies of the most actively transcribed early genes. Regions adjacent to the terminal redundancy are also transcribed at early times but at a much lower level. A small amount of early RNA synthesis can also be detected on *Eco*RI* fragment 3, in the center of the genome. This could represent transcription of regulatory gene *28*, an early gene located in this region of the physical map, whose product activates middle gene transcription.

Genes that are expressed at middle times are located over much of the phage genome, with the most actively transcribed middle genes clustered in two areas: one area just to the right of the center of the physical map and the other area adjacent to the redundant region at the left end of the map. Active transcription of both of these regions requires the gene *28* product. Finally, the region of the genome just to the left of center is expressed only at late times; transcription of these genes requires the products of both gene *33* and gene *34*.

In the absence of nucleoside triphosphates, RNA polymerase binds strongly to promoter sites on DNA to form stable binary complexes that can be isolated on nitrocellulose filters. We have previously used this filter binding assay to determine which of the *Eco*RI* restriction fragments contained promoters for either the unmodified bacterial RNA polymerase or the SP01-modified RNA polymerase containing the gene *28* product (19). In Fig. 9 the asterisks above fragments containing early genes indicate the *Eco*RI* fragments specifically and most actively bound by the bacterial RNA polymerase, whereas the asterisks above fragments containing middle genes show the restriction fragments with strongest promoters for the phage-modified transcriptase containing the gene *28* protein. (Several other fragments which hybridized labeled RNA and which bound RNA polymerase weakly are not designated with asterisks in Fig. 9). In all cases, fragments with early or middle promoters corresponded to DNA segments that contained early or middle sequences, respectively. However, a few fragments that were actively transcribed at early or middle times did not have DNA binding sites (e.g., fragment 21). We presume that these DNA segments are transcribed by "read-through" from adjacent segments with promoters.

Although this analysis has permitted us for the first time to assign early, middle, and late sequences to general regions on the phage genome, the detailed identification of units of tran-

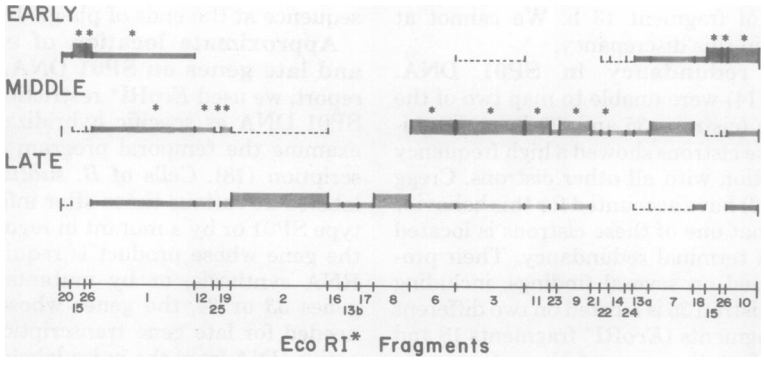

FIG. 9. *General locations of early, middle, and late sequences on the SP01 genome. The thick, thin, or dotted lines represent the relative amounts of early, middle, or late labeled RNA that hybridized to each of the indicated EcoRI* restriction fragments. These hybridization data are derived from the study of Talkington and Pero (18) as described in the text. Asterisks indicate fragments that have strong promoters for either the unmodified bacterial RNA polymerase (early line) or the SP01-modified enzyme containing the gene 28 protein (middle line) (19). Since EcoRI* fragments 13a and 13b, as well as fragments 14 and 15, were not resolved on the Southern strips of our previous hybridization studies, we have arbitrarily assigned the hybridized RNA to one (or both) member(s) of each pair of DNAs on the basis of the amount of RNA hybridizing to restriction fragments neighboring each member of the pair.*

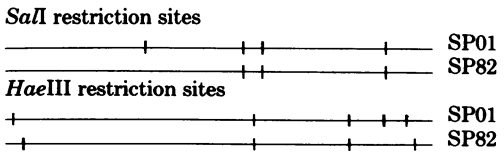

FIG. 10. *Comparison of SalI and HaeIII cleavage maps of phages SP01 and SP82.*

scription must await a higher resolution map of the location and orientation of promoter sites for unmodified and phage-modified polymerases.

Comparing the restriction maps of SP01 and SP82 DNAs. Lawrie and Whiteley (11) have mapped the recognition sites for the restriction endonucleases *SalI* and *HaeIII* on the DNA of phage SP82, a close relative of SP01. In addition, they have compared the sizes of SP82 fragments generated by *HaeIII* or *SalI* with the sizes of the SP01 fragments generated by these same restriction enzymes (9). In Fig. 10 we compare the *SalI* and *HaeIII* cleavage maps of these two phages. As expected, some but not all of the *SalI* and *HaeIII* cut sites in SP82 DNA appear to correspond in location to those in SP01 DNA. In addition, Lawrie and Whiteley (11) have grouped the large number of fragments produced by *HpaII* digestion of SP82 DNA into general regions of the phage genome as defined by a *HaeIII-SalI* map. In view of our demonstration of terminal redundancy in SP01 DNA, it is interesting to note that five of the *HpaII* fragments of Lawrie and Whiteley (fragments 28, 29, 30, 33, and 37) seem to be present in *HaeIII-SalI* fragments from both ends of the genome. Thus, like its close relative, SP82 DNA could be terminally redundant; however, the *HpaII* restriction fragments will have to be ordered to establish this point. Hybridizations of SP82 RNA to the separated *HpaII* fragments indicated that SP82 early genes, like those of SP01, are located at the ends of the phage genome; but distinct regions for SP82 middle and late genes could not be discerned (10). As more detailed information becomes available on the structure of SP82 and SP01 DNAs, it will be of interest to compare the organization of temporally regulated genes on the two phage genomes.

ACKNOWLEDGMENTS

We thank Richard Losick for help in the preparation of this manuscript.

This work was supported by National Science Foundation grant PCM75-00551 A01 To J.P.

LITERATURE CITED

1. **Cregg, J. M., and C. R. Stewart.** 1978. *Eco*RI cleavage of DNA from *Bacillus subtilis* phage SP01. Virology **85**:601–605.
2. **Cregg, J. M., and C. R. Stewart.** 1978. Terminal redundancy of "high frequency of recombination" markers of *Bacillus subtilis* phage SP01. Virology **86**:530–541.
3. **Duffy, J. J., and E. P. Geiduschek.** 1977. Purification of a positive regulatory subunit from phage SP01-modified RNA polymerase. Nature (London) **270**:28–32.
4. **Fox, T. D.** 1976. Identification of phage SP01 proteins coded by regulatory genes *33* and *34*. Nature (London) **262**:748–753.
5. **Fox, T. D., R. Losick, and J. Pero.** 1976. Regulatory gene *28* of bacteriophage SP01 codes for a phage-induced subunit of RNA polymerase. J. Mol. Biol. **101**: 427–433.
6. **Fujita, D. J., B. M. Ohlsson-Wilhelm, and E. P. Geiduschek.** 1971. Transcription during bacteriophage SP01 development: Mutations affecting the program of viral transcription. J. Mol. Biol. **57**:301–317.
7. **Hamlett, N. V., B. Lange-Gufstafson, and M. Rhoades.** 1977. Physical map of the bacteriophage T5 genome based on the cleavage products of the restriction endonucleases *SalI*, *SmaI*, *BamI*, and *HpaI*. J. Virol. **24**:249–260.
8. **Ito, J., F. Kawamura, and J. J. Duffy.** 1975. Susceptibility of non-thymine containing DNA to four bacterial restriction endonucleases. FEBS Lett. **55**:278–281.
9. **Lawrie, J. M., J. S. Downard, and H. R. Whiteley.** 1978. *Bacillus subtilis* bacteriophages SP82, SP01, and ϕe: a comparison of DNAs and of peptides synthesized during infection. J. Virol. **27**:725–737.
10. **Lawrie, J. M., G. B. Spiegelman, and H. R. Whiteley.** 1977. Localization of transcripts produced *in vivo* and *in vitro* on phage SP82 genome. Gene **2**:251–262.
11. **Lawrie, J. M., and H. R. Whiteley.** 1977. A physical map of bacteriophage SP82 DNA. Gene **2**:233–250.
12. **McDonell, M. W., M. N. Simon, and F. W. Studier.** 1977. Analysis of restriction fragments of T7 DNA and determination of molecular weights by electrophoresis in neutral and alkaline gels. J. Mol. Biol. **110**:119–146.
13. **Okubo, S., B. Strauss, and M. Stodolsky.** 1964. The possible role of recombination in the infection of competent *Bacillus subtilis* by bacteriophage deoxyribonucleic acid. Virology **24**:552–562.
14. **Okubo, S., T. Yanagida, D. J. Fujita, and B. M. Ohlsson-Wilhelm.** 1972. The genetics of bacteriophage SP01. Biken J. **15**:81–97.
15. **Polisky, B., P. Green, D. E. Garfin, B. J. McCarthy, H. M. Goodman, and H. W. Boyer.** 1975. Specificity of substrate recognition by the *Eco*RI restriction endonuclease. Proc. Natl. Acad. Sci. U.S.A. **72**:3310–3314.
16. **Sanger, F., G. M. Air, B. G. Barnell, N. L. Brown, A. R. Coulson, J. C. Fiddes, C. A. Hutchison III, P. M. Slocombe, and M. Smith.** 1977. Nucleotide sequence of bacteriophage ϕX174 DNA. Nature (London) **265**: 687–695.
17. **Southern, E. M.** 1975. Detection of specific sequences among DNA fragments separated by gel electrophoresis. J. Mol. Biol. **98**:503–517.
18. **Talkington, C., and J. Pero.** 1977. Restriction fragment analysis of the temporal program of bacteriophage SP01 transcription and its control by phage-modified RNA polymerases. Virology **83**:365–379.
19. **Talkington, C., and J. Pero.** 1978. Promoter recognition by phage SP01-modified RNA polymerase. Proc. Natl. Acad. Sci. U.S.A. **75**:1185–1189.
20. **Thomas, M., and R. W. Davis.** 1975. Studies on the cleavage of bacteriophage lambda DNA with *Eco*RI restriction endonuclease. J. Mol. Biol. **91**:315–328.
21. **Tjian, R., and J. Pero.** 1976. Bacteriophage SP01 regulatory proteins directing late gene transcription *in vitro*. Nature (London) **262**:753–757.